International Journal of Terraspace Science and Engineering 8(2)2016 75-82

Multiscale fracture of cellular materials

Liviu Marsavina [a,*], Emanoil Linul [a]

[a] *Department of Mechanics and Strength of Materials, University Politehnica Timisoara, Timisoara, ROMANIA*

Abstract

This paper presents a review of mode I fracture toughness obtained by authors from micromechanical modeling and fracture toughness test. The multiscale approach starts from cellular parameters (relative density, cell dimensions, cell topology) using micromechanical analytical or numerical models, which could be validated by classic fracture toughness test and finally extrapolated to large structures via size effect. A 2D solid representative volume was considered for numerical simulations and the fracture toughness was determined from the fracture strength of the first strut in front of the crack. The mode I fracture toughness was determine using three different specimens (Single Edge Notch Bending, Single Edge Crack and Asymmetric Semi Circular Bending). Different Polyurethane foam densities were investigated. Finally, a good correlation between analytical, numerical and experimental fracture toughness results was obtained.

***Keywords*:** *Multiscale fracture; Cellular material.*

1. Introduction

Cellular materials are widely used in applications like heat exchangers and thermal protection systems, in military and commercial aerospace structures, in large portable structures and flotation devices, in composite sandwich structures [1-3].

One important class of multiscale analysis starts from microscopic trough mesoscopic and macroscopic scale and ends to components and structures. In many practical problems, chemical compositions of materials have already been fixed and the effects of electronic and atomic structure is clear, thus the property of the materials depends further on their microstructure in the continuum domain. The main purpose in this case of multiscale analysis is to derive the relationship between property and structure hierarchy, and it usually spans microscopic, mesoscopic and macroscopic scales of continuum [4].

For the case of cellular materials at microscopic scale is the structure of solid materials from cells edges and struts, at mesoscale the main features are the topology of cells (shape, dimensions, arrangements) and at macroscale the properties of cellular material. They all influence the behavior of components or structures incorporating the cellular material. Fig. 1 presents an example for Polyurethane (PUR) foam, at microscale we have the structure of polyurethane (a), at mesoscale the structure of cells (b), at macroscopic scale the testing specimens, in this case a shear specimen for Iosipescu test (c), and finally a wing composite structure with face made of carbon fiber reinforced polymer and a PUR foam core (d).

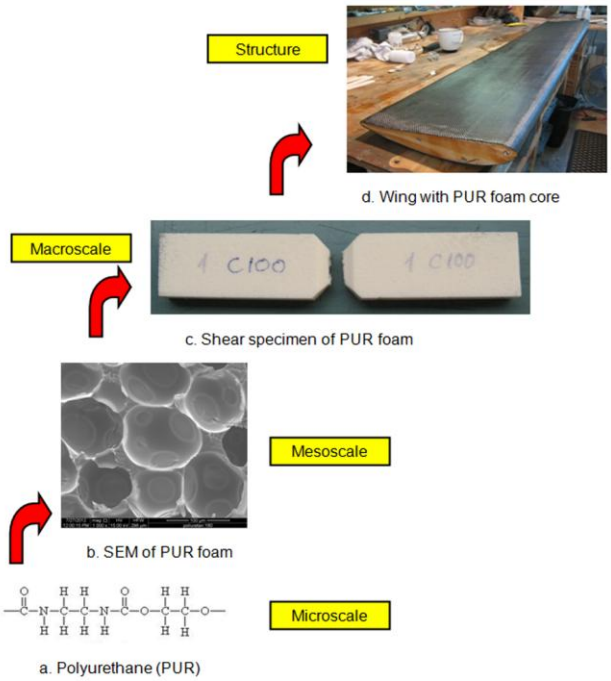

Fig.1 Hierarchy of multiscale analysis for PUR foam used as core in wing.

Mechanical properties could also be experimentally determined trough mechanical testing in compression [5,6], tensile [7-9], bending [10,11], shear [12], fracture toughness [13-15], fatigue [16,17]. Finally, the behavior of composite structure should be investigated.

Different researchers presented different aspects of evaluation of fracture and failure of cellular materials, like micromechanical models, numerical simulations, experimental determination of fracture toughness [18-20]. This paper will review some of them, and also will present a comprehensive multiscale approach

*Corresponding author.
E-mail address: liviu.marsavina@upt.ro

applied to PUR foams starting from microstructural topology to macroscopic evaluation of fracture toughness.

2. Microstructure of Polyurethane foams

In this paper the focus will be on Polyurethane (PUR) foams representing an important class of cellular materials. Fig. 2 presents several microstructures of PUR foams, all belong to rigid foams having a closed cell structure. It could be observed three different cell topologies: a. rectangular (40 kg/m^3), b. hexagonal (100 kg/m^3) and c. circular (300 kg/m^3) cells.

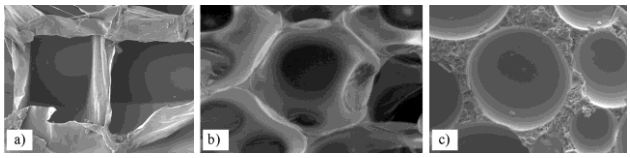

Fig. 2 Typical microstructures of rigid PUR foams with closed cells: with square (a), hexagonal (b) and circular (c) shapes.

Alongside with cell topology the relative density of foam, which represents the ratio between the foam density to that of the solid material ρ^*/ρ_s is the most important microstructure feature. Relative density influences the mechanical properties of foam.

3. Micromechanical models to predict fracture toughness of cellular materials

Micromechanical models are used at mesoscale level to predict mechanical properties of cellular materials [19,20]. These models predict the fracture toughness of cellular material K_{Ic} to the fracture strength of the cell walls σ_{fs}, cell length dimension l, and the relative density ρ^*/ρ_s having the general form:

$$\frac{K_{IC}}{\sigma_{fs}\sqrt{\pi l}} = C\left(\frac{\rho^*}{\rho_s}\right)^n . \quad (1)$$

where C=0.65 is a constant of proportionality provided in by comparison with some experimental data, and n=1.5 [1].

For the fracture toughness the models were developed by assuming that the crack tip is located at half-edge length and considered an elastic mode I stress field at the crack tip. The singular stress field at the tip of a crack of length $2a$ and normal to remote loading σ in an elastic continuum solid was considered. It was assumed that the fracture occurs when the ultimate tensile strength was reached in the first strut ahead of the crack, placed at distance r (on a direction θ = 0) from crack tip. It was considered only the singular term in the Irwin's stress field solution, and only the bending of struts.

Choi and Lakes [21] proposed a micromechanical model taking into account the blunting at the crack tip, and corresponding nonsingular stress field. A linear expression between non-dimensional fracture toughness and relative density was obtained (n=1) and C=0.19.

Similar correlation was proposed by Green [22] considering elastic deformation in shell theory of hollow sphere model for foam cells. For this model C=0.28 and n = 1.3 values were found.

Choi and Shakar [23] takes into account that the struts in front of the crack are subjected to a combined load (bend and tensile) and equal the resulting stress with the tensile strength of the solid σ_{fs}, assuming the singular solution at the crack tip. In the predicted fracture toughness relation appears crack length a in contrast with the other solutions. A mode II fracture toughness solution was also proposed.

4. Micromechanical models based on finite element analysis

Finite element modelling methods are used to describe the behaviour and mechanical properties of cellular structures Lipperman et al. [24], Daxner [25]. Fleck and Qiu [26] have determined fracture toughness of elastic-brittle 2D lattices by the finite element method for three isotropic periodic topologies: the regular hexagonal honeycomb, the Kagome lattice and the regular triangular honeycomb. Also, a finite element based method developed by Choi and Sankar [23] has been used by Wang [27] to study the fracture toughness of two types of foams: with rectangular prism unit cells, including homogeneous foams and functionally graded foams, and tetrakaidecahedral foams. He obtained the plain-strain fracture toughness of the foam by relating the fracture toughness to the tensile strength of the cell struts. Most of the models considered the cell struts as beams, for open cells, or shells for closed cells. Recently, a novel 2D solid rectangular micromechanical finite element model was proposed by Linul and Marsavina [19] for predicting the fracture toughness of cellular polymers for both Modes I and II of loading.

The Mode I fracture toughness using Finite Element micromechanical models was determined increasing the applied load σ until the maximum stress $\sigma_{y,max}$ in the first unbroken strut reaches the fracture strength of the solid material σ_{fs}.

A Central Cracked Plate (CCP) specimen under Tension was considered. The Mode I fracture toughness of cellular material was estimated:

$$K_{IC} = \sigma_{fs}\sqrt{\pi a}\, f_I(a/W) \quad (2)$$

where a [mm], represents the half of crack length, W [mm] width of the model and $f_I(a/W)$ a

non-dimensional function from stress intensity factors handbooks [28, 29]:

$$f_I\left(\frac{a}{W}\right)=\frac{1-0.5\left(\frac{a}{W}\right)+0.37\left(\frac{a}{W}\right)^2-0.044\left(\frac{a}{W}\right)^3}{\sqrt{1-\left(\frac{a}{W}\right)}}. \quad (3)$$

Due to symmetry of CCP specimen a quarter of the specimen was modelled in plane strain conditions. The struts of the cells were considered as 2D solids. The simulations were carried on FRANC2D/L software, using quadratic 8 nodes plane strain elements. The mechanical characteristics of PUR solid material were: density ρ_s=1170 kg/m^3, Young's modulus E=1600 MPa, Poisson's ratio ν=0.40 and fracture strength σ_{fs}=130 MPa.

The numerical models of different cell topology are shown in Fig. 3.

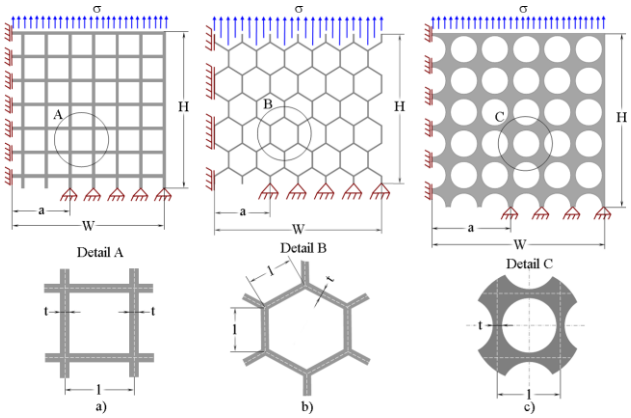

Fig. 3 FE micromechanical models and applied boundary conditions for a. square, b. honeycomb and c. circular cells.

The symmetric boundary conditions were imposed, and the load was applied perpendicular to the crack, in order to produce a Mode I loading. The crack was inserted by breaking the ligaments of the cells in the crack area [1].

A convergence study was carried on in order to find the optimum model size. Fig.4.a presents the variation of estimated fracture toughness versus the number of cells and Fig. 4.b presents the influence of the crack length. It could be observed that a model with 64 cells is a representative volume for simulating the cellular structure. The crack length doesn't influence the value of K_{IC}, which could be assumed as a material property.

The obtained results from FEA micromechanical modeling on fracture toughness are summarized in Table 1.

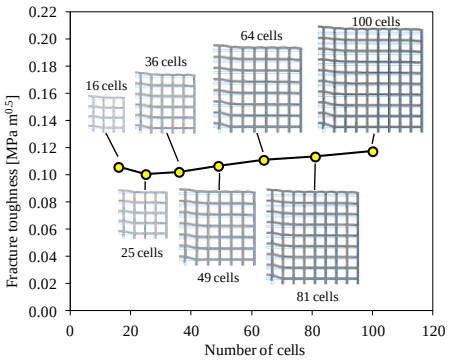

a. Influence of the number of cells

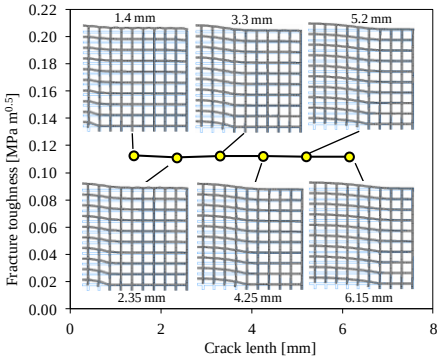

b. Influence of the crack length

Fig. 4 Convergence study results.

Table 1 Mode I fracture toughness results

l [mm]	t [mm]	ρ^*/ρ_s [-]	Cell topology	K_{IC} $[MPa\sqrt{m}]$
0.52	0.02	0.077	Rectangular	0.051
0.95	0.05	0.105	Rectangular	0.112
0.75	0.05	0.133	Rectangular	0.141
0.55	0.05	0.182	Rectangular	0.186
0.60	0.10	0.333	Rectangular	0.384
0.35	0.10	0.333	Honeycomb	0.402
0.50	0.10	0.502	Circular	0.472

5. Experimental determination of fracture toughness

At macroscale the fracture toughness of PUR foams could be determined following the standard procedure of determination of fracture toughness for solid plastic materials [30]. Different studies could be found in literature for mode I [31-35], mode II [12] and mixed mode [36,37] fracture of cellular materials. Present paper review the fracture toughness results obtained by authors for PUR foams.

Three types of specimens were considered for mode I and mixed mode fracture toughness determination of PUR foams. Table 2 summarize the specimens and stress intensity factor solutions.

Table 2 Specimens and stress intensity factors solutions

Specimen type: SENB

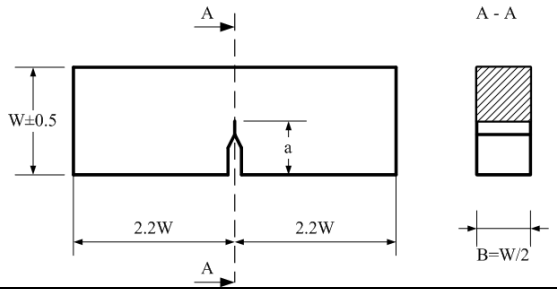

$$K_{IC}=\frac{3P_{max}\,S}{2B\,W^2}\,f(a/W), \qquad \text{Ref. [15]}$$

$$f(a/W)=1.122-1.40(a/W)+7.33(a/W)^2-13.08(a/W)^3+14.0(a/W)^4$$

Specimen type: SEC

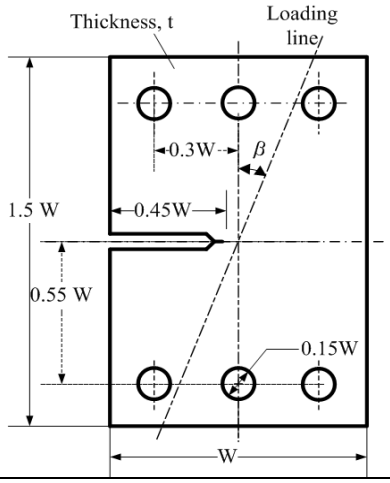

$$K_i=\frac{P_{max}}{W\,t}\sqrt{\pi a}\;f_i(\beta,a/W),i=I,II \qquad \text{Ref. [45]}$$

$$f_I(\beta,a/W)=\frac{\cos\beta}{1-\frac{a}{W}}\sqrt{\frac{0.26+2.65\frac{a}{W-a}}{1+0.55\frac{a}{W-a}-0.88\left(\frac{a}{W-a}\right)^2}}$$

$$f_{II}(\beta,a/W)=\frac{\sin\beta}{1-\frac{a}{W}}\sqrt{\frac{-0.23+1.40\frac{a}{W-a}}{1-0.67\frac{a}{W-a}+2.08\left(\frac{a}{W-a}\right)^2}}$$

Specimen type: ASCB

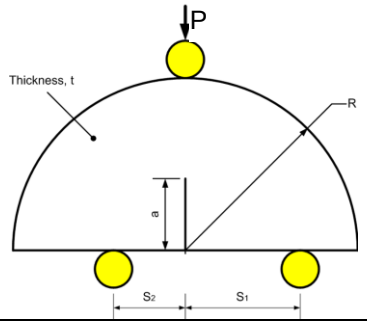

$$K_i=\frac{P_{max}}{2Rt}\sqrt{\pi a}\;f_i(a/R,S_1/R,S_2/R), \quad i=I,II \qquad \text{Ref. [41]}$$

$$f_I(S_2/R)=6.235(S_2/R)^3-15.069(S_2/R)^2+17.229(S_2/R)-1.062$$

$$f_{II}(S_2/R)=1.884(S_2/R)^5-7.309(S_2/R)^4+5.037(S_2/R)^3+2.77(S_2/R)^2-5.075(S_2/R)+1.983$$

The Single Edge Notched Bend (SENB) specimen, loaded in three point bending produces mode I conditions [15]. The dimensions of the SENB specimens were W = 25 mm, B = 12.5 mm and a = 12 mm.

The Single Edge Crack (SEC) specimen with Arcan grips can produce from pure mode I to pure mode II only by changing the loading angle, β [27]. The dimensions of the SEC specimens were W = 75 mm, t = 8 mm and a = 33.75 mm and the loading angle was $\beta = 0^0$ for mode I tests.

The Asymmetric Semi-Circular Bend (ASCB) specimen, was also used to perform mode I and mixed mode fracture toughness tests [28]. This semi-circular specimen with radius R, which contains an edge crack of length a oriented normal to the specimen edge, loaded with a three point bend fixture, was proved to give a wide range of mixed modes from pure mode I (S_1=S_2) to pure mode II (S_1≠S_2), only by changing the position of one support. The considered geometry of the specimen has: R=40 mm, a=20 mm, t=10 mm, S_1=30 mm for symmetric loading and mode I fracture toughness determination and S_2=2.66 mm for mode II fracture toughness determination.

The stress intensity factor solutions are also presented in Table 2. For SENB and SEC specimens the solutions were provided in literature [15, 27], while for the ASCB specimen were determine using finite element analysis [29].

The load - displacement curves show a linear elastic behavior and a brittle fracture without any plastic deformations [15, 27, 28].

The mode I fracture toughness average results obtained experimentally are summarized in Table 3 together with average cell size and density.

Table 3 Mode I Fracture toughness - experimental results

Spec. type	l [μm]	ρ^* [kg/m^3]	K_{IC} [$MPa\sqrt{m}$]	Ref.
SENB	198.6	40	0.032	[13-15, 18]
	163.7	80	0.058	[15]
	104.5	100	0.089	[13, 15, 46]
	175.2	120	0.121	[15]
	377.1	140	0.153	[13, 15, 18]
	83.8	145	0.131	[13, 15, 46]
	333.6	200	0.39	[18]
	68.5	300	0.372	[13,46]
	70.8	480	1.11	[48]
	83.5	540	1.25	[48]
	65.3	600	1.34	[48]
	49.1	620	1.46	[48]
SEC	104.5	100	0.088	[45]
	83.8	145	0.109	[45]
	68.5	300	0.337	[45]
ASCB	104.5	100	0.087	[45-47]
	83.8	145	0.131	[45-47]
	68.5	300	0.372	[45-47]

It could be observed that the fracture toughness increases with density from 0.032 $MPa\sqrt{m}$ for foam

with density 40 kg/m^3 to 1.46 $MPa\sqrt{m}$ kg/m^3 for foam density 620 kg/m^3. The specimen shape does not influence the K_{IC} value, which indicates that the fracture toughness is a material parameter.

The SEC and ASCB specimens allow the determination of mixed mode fracture, only by changing the loading angle β for SEC, respectively the distance S_2 for ASCB. The obtained results, expressed by the ratio between K_{II}/K_{IC} versus K_I/K_{IC} for three different densities are compared with four classical fracture criteria: Maximum Tensile Stress (MTS) [38], Strain Energy Density (SED) [39], Maximum Energy Release Rate (Gmax) [40] and Equivalent Stress Intensity Factor (ESIF) [41,42], Fig. 5. It could be observed that for low density foams (100 and 145 kg/m^3) Gmax and ESIF criteria predicted better the fracture, while for the foam with 300 kg/m^3 the SED fracture envelope curve provide the close estimates. Similar results were obtained by Noury et al. [37] on foams of 90, 130 and 200 kg/m^3 densities. This could be explained that higher density foam has a porous solid structure rather than a cellular one and the SED fracture criteria fits better the experimental fracture toughness results.

Both specimen types ASCB and SEC give close predictions for mixed mode fracture.

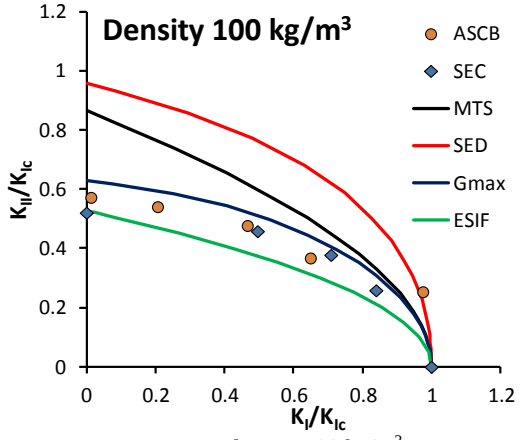

a. Foam density 100 kg/m^3

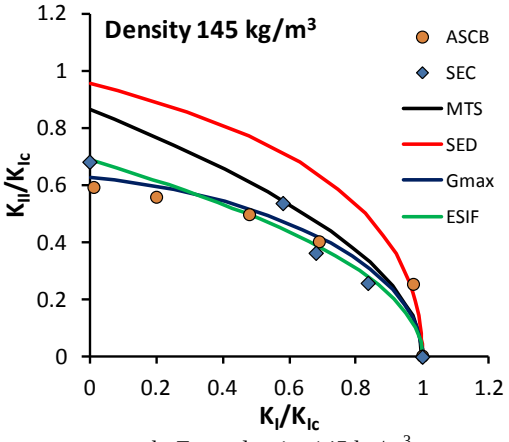

b. Foam density 145 kg/m^3

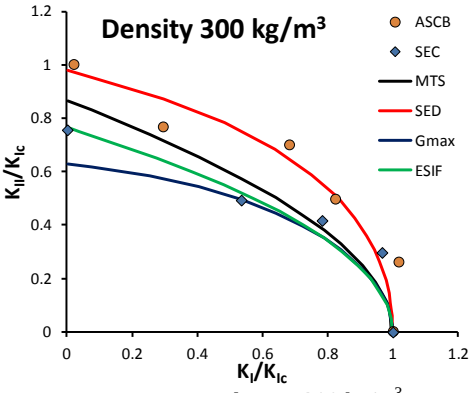

c. Foam density 300 kg/m^3

Fig. 5 Experimental results for mixed mode fracture using ASCB and SEC specimens and fracture envelope curves.

Size effect on cellular materials was investigated by Bazant et al. [43, 44].

For transferring the data to a large scale structure a size effect study was preformed. All investigated SENB specimens were prepared from the same plate with thickness of approximately 53 mm for foam densities 100 and 145 kg/m^3, and 25 mm for 300 kg/m^3 density [13]. The width of specimens was kept constant, and five sizes of the specimen width were considered: XS-Extra Small, S-Small, M-Medium, L-Large and XL-Extra Large. Also, the ratio between span to width (S/W = 4) and the ratio between crack length to width (a/W=0.5) were constant.

Table 4 Size effect - experimental results

ρ^* [kg/m^3]	Spec. size	B [mm]	W [mm]	σ_N [MPa]	K_{IC} [$MPa\sqrt{m}$]
100	XS	53.12	5.38	0.567	0.071
	S	53.30	10.11	0.491	0.087
	M	53.31	25.45	0.317	0.089
	L	53.69	100.19	0.171	0.096
	XL	53.27	224.50	0.110	0.093
145	XS	52.17	5.55	0.834	0.105
	S	52.30	10.79	0.759	0.135
	M	52.23	25.94	0.475	0.133
	L	51.72	100.84	0.244	0.137
	XL	51.83	226.6	0.155	0.131
300	XS	25.37	5.65	2.957	0.375
	S	25.33	10.58	2.211	0.392
	M	25.31	25.57	1.367	0.383
	L	25.27	87.97	0.688	0.361
	XL	25.30	173.65	0.476	0.354

The experimental data are plotted in terms of *Log* σ_N versus *Log* W (Fig. 6), where for SENB specimen W represents the width and

$$\sigma_N = \frac{3P_{max}\,S}{2BW^2} \tag{4}$$

is the stress in bending specimen at failure load. Also in Fig. 6 are plotted the stress condition (ductile

behaviour with no size effect) for which $\sigma_N = \sigma_{yield}$ (horizontal black point line) and a brittle behavior according to the Linear Elastic Fracture Mechanics (LEFM) condition (dashed red line with slope -0.5). The experimental results could be better described by an asymptotic representation (solid black line) to these two lines, having the form:

$$\sigma_N = \frac{\sigma_{N0}}{\sqrt{1+\frac{W}{W_0}}}. \quad (5)$$

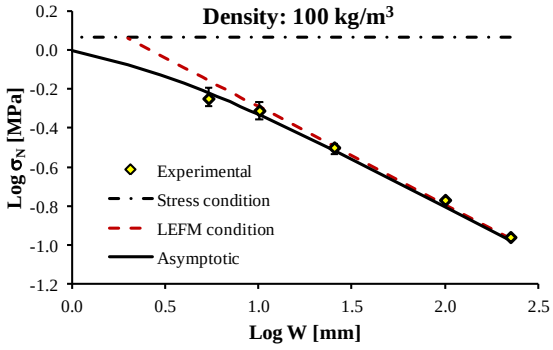

a. Foam density 100 kg/m^3

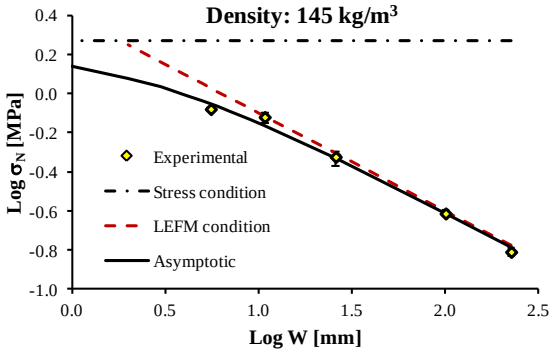

b. Foam density 145 kg/m^3

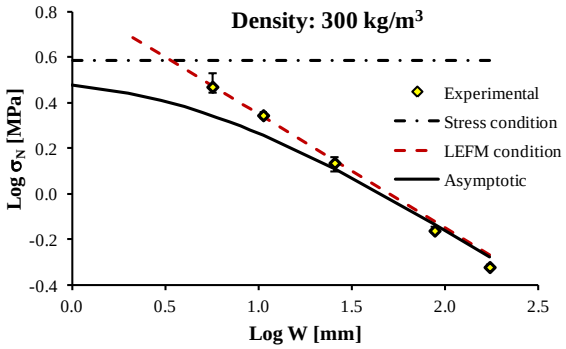

c. Foam density 300 kg/m^3

Fig. 6 Size effect results for PUR foams using similar SENB specimens.

The fitting parameters were obtained by numerical interpolation. In Fig. 6 it could be observed that only for low density foams (100 and 145 kg/m^3 density) and specimens with the lowest specimen width 5 mm doesn't respect the LEFM condition. All the other specimen sizes are in the validity of LEFM.

6. Conclusions

The paper presents a review of fracture toughness of PUR foams linking the microscale to macroscale.

To summarize in Fig. 7 are plotted together the experimental and numerical predicted normalized fracture toughness results, and the micromechanical model described by eq. (1). It could be a good correlation between the obtained results.

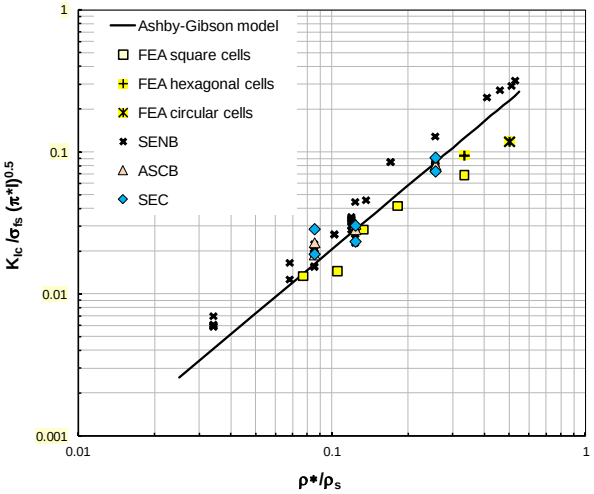

Fig.7 Comparison between micromechanical models and experimental results for K_{IC} for PUR foams.

The main conclusions are:

- relative density of the foam represents the main parameter influencing the fracture toughness. The cell topology has little influence.
- the micromechanical models could predict accurate values of fracture toughness.
- Finite Element models which could represent the cellular structures are useful tools for estimation of mechanical properties.
- micromechanical models could be validated using fracture toughness tests at macroscopic level.
- the fracture criteria developed for continuum isotropic materials could be successfully applied to cellular materials to evaluate the mixed mode fracture.
- transfer of results at large scale components could be carried on taking into account the size effect.

Acknowledgement

Part of the numerical and experimental results presented were obtained in the framework of Grant PN-II-ID-PCE-2011-3-0456, contract number 172/2011 financed by the CNCS – UEFISCDI.

References

[1] L.J. Gibson, M.F. Ashby, Cellular Solids-Structures and properties-Second edition, Published by the Press Syndicate of the University of Cambridge (1997).

[2] E. Linul and L. Marsavina, Assesment of sandwich beams with rigid polyurethane foam core using failure-mode maps, Proceedings of the Romanian Academy – Series A, 16(4) (2015) 522-530.

[3] M. Birsan, T. Sadowski, L. Marsavina, E. Linul, and D. Pietras, Mechanical behavior of sandwich composite beams made of foams and functionally graded materials, International Journal of Solids and Structures, 50 (2013) 519-530.

[4] J. Fan, Multiscale analysis of deformation and failure of materials, John Wiley & Sons, Ltd, Chichester (2011).

[5] E. Linul, T. Voiconi, L. Marsavina, T. Sadowski, Study of factors influencing the mechanical properties of polyurethane foams under dynamic compression, Journal of Physics: Conference Series 451 (2013) 1-6.

[6] D.A. Apostol, D.M. Constantinescu, L. Marsavina, E. Linul, Analysis of Deformation Bands in Polyurethane Foams, Key Engineering Materials, 601 (2014) 250-253.

[7] R. Negru, L. Marsavina, T. Voiconi, E. Linul, H. Filipescu, G. Belciu, Application of TCD for brittle fracture of notched PUR materials, Theoretical and Applied Fracture Mechanics, vol. 80, Part A (2015) 87-95.

[8] T. Voiconi, R. Negru, E. Linul, L. Marsavina, H. Filipescu, The notch effect on fracture of polyurethane materials, Fracture and Structural Integrity, 30 (2014) 101-108.

[9] L. Marsavina, J. Kováčik, E. Linul, Experimental validation of micromechanical models for brittle aluminium alloy foam, Theoretical and Applied Fracture Mechanics (2016), doi: http://dx.doi.org/ 10.1016/j.tafmec.2015.12.020

[10] T. Voiconi, E. Linul, L. Marsavina, T. Sadowski, M. Knec, Determination of flexural properties of rigid PUR foams using digital image correlation, Solid State Phenomena, 216 (2014) 116-121.

[11] D. A. Apostol, D. M. Constantinescu, L. Marsavina, E. Linul, Mixed-Mode Testing for an Asymmetric Four-Point Bending Configuration of Polyurethane Foams, Applied Mechanics and Materials, 760 (2015) 239-244.

[12] L. Marsavina, D.M. Constantinescu, E. Linul, T. Voiconi, D.A. Apostol, Shear and mode II fracture of PUR foams, Engineering Failure Analysis, 58 (2015) 465-476.

[13] L. Marsavina, D.M. Constantinescu, E. Linul, D.A. Apostol, T. Voiconi, T. Sadowski, Refinements on fracture toughness of PUR foams, Engineering Fracture Mechanics, 129 (2014) 54-66..

[14] E. Linul, L. Marsavina, T. Sadowski and M. Kneć, Size Effect on Fracture Toughness of Rigid Polyurethane Foams, Solid State Phenomena 188 (2012) 205-210.

[15] L. Marsavina, E. Linul, T. Voiconi, T. Sadowski, A comparison between dynamic and static fracture toughness of polyurethane foams, Polymer Testing, 32 (2013) 673-680.

[16] A. Bezazi, F. Scarpa, Tensile fatigue of conventional and negative Poisson's ratio open cell PU foams, International Journal of Fatigue, 31 (2009) 488–494.

[17] S. Demiray, W. Becker, J. Hohe, Investigation of the fatigue behavior of open cell foams by a micromechanical 3-D model, Materials Science and Engineering A, 504 (2009) 141–149.

[18] L. Marsavina, E. Linul, Fracture toughness of polyurethane foams. Experimental versus micromechanical models, Fracture of Materials and Structures from Micro to Macro Scale, The 18th European Conference on Fracture, Dresden, Germany, August 30-September, 03, 2010.

[19] E. Linul and L. Marsavina, Prediction of fracture toughness for open cell polyurethane foams by finite element micromechanical analysis, Iranian Polymer Journal, 20(9) (2011) 736-746.

[20] A. Șerban, E. Linul, T. Voiconi, L. Marsavina, N. Modler, Numerical evaluation of two-dimensional micromechanical structures of anisotropic cellular materials: case study for polyurethane rigid foams, Iranian Polymer Journal, 24 (2015) 515-529.

[21] J.B. Choi, R.S. Lakes, Fracture Toughness of Re-entrant Foam Material with a Negative Poisson's Ratio: Experimental and Analysis, International Journal of Fracture 80 (1996) 73-83.

[22] D.J. Green, Fabrication and Mechanical Properties of Lightweight Ceramics Produced by Sintering of Hollow Spheres, Journal of the American Ceramic Society 68 (1985) 403-409.

[23] S. Choi, B.V. Sankar, A micromechanical method to predict the fracture toughness of cellular materials. International Journal of Solids and Structures 42 (2005) 1797-1817.

[24] F. Lipperman, M. Ryvkin, M. Fuchs M Fracture toughness of two-dimensional cellular material with periodic microstructure. Int J Fract 146 (2007) 279–290.

[25] T. Daxner, Finite element modelling of cellular materials. In: Altenbach H, Ochsner A (Eds) Cellular and porous materials in structures and processes, Springer (2010).

[26] N.A. Fleck, X. Qiu X The damage tolerance of elastic-brittle, two dimensional isotropic lattices. J Mech Phys Solids 55(3) (2007) 562-588.

[27] J. Wang, Fracture toughness of cellular materials using finite element based micromechanics. A dissertation presented to the University of Florida, Florida (2007).

[28] H. Tada, P.C. Paris, G. R. Irwin, The stress analysis of cracks handbook, 3rd Edition, ASME, New York, (2000).

[29] W. T. Koitier, Note on Stress Intensity Factor for Sheet Strips with Cracks under Tensile Loads, Report No. 314, University of Technology Delft, (1965).

[30] ASTM D5045-99: Standard Test Methods for Plane-Strain Fracture Toughness and Strain Energy Release Rate of Plastic materials.

[31] L. Marsavina L. Fracture Mechanics of Cellular Solids. In: H. Altenbach, A. Ochsner, editors. Cellular and porous materials in structures and processes, Wien: Springer; 2010.

[32] C.W. Fowlkes, Fracture toughness of a rigid polyurethane foam, Int J Fract 10(1) (1974) 99-108.

[33] G.M. Viana, L.A. Carlsson, Mechanical properties and fracture characterisation of cross-linked PVC foams, J Sandw Struct Mater, 4 (2002) 99-113.

[34] M. Burman, Fatigue crack initiation and propagation in sandwich structures, Report No.98-29, Stockholm (1998).

[35] M.E. Kabir, M.C. Saha, S. Jeelani, Tensile and fracture behavior of polymer foams, Mat Sci Eng, A 429 (2006) 225-235.

[36] S. Hallstrom, J.L. Grenestedt, Mixed mode fracture of cracks and wedge shaped notches in expanded PVC foam, I. J. Fract, 88 (1997) 343-358.

[37] P.M. Noury, R.A. Shenoi, I. Sinclair, On mixed-mode fracture of PVC foam, I J Fract, 92 (1998)131-151.

[38] F. Erdogan, G.C. Sih, On the crack extension in plates under plane loading and transverse shear. J Basic Engn, 85 (1963) 519-525.

[39] G.C. Sih, Strain-energy-density factor applied to mixed mode crack problems, I J Fract, 10 (1974) 305-321.
[40] M.A. Hussain, S.L. Pu, J. Underwood, Strain energy release rate for a crack under combined mode I and mode II. In: Fracture analysis, Paris PC, G.R. Irwin GR Editors, ASTM STP560, Philadelphia, 2-28 (1974).
[41] H.A. Richard, *Bruchvorhersagen bei ueberlagerter Normal- und Schubbeanspruchung von Rissen*, VDI-Verlag, Dusseldorf (1985).
[42] H.A. Richard, M. Fulland, M. Sander, Theoretical crack path prediction, Fatigue Fract Engng Mater Struct, 28 (2005)3-12.
[43] Z. P. Bažant Scaling of Structural Strength, London: Hermes-Penton; 2002.
[44] Z. P Bažant, Z. Yong, Z. Goangseup Z, M.D. Isaac, Size effect and asymptotic matching analysis of fracture of closed-cell polymeric foam, I J Solis Struct 2003; 40: 7197–7217.
[45] L. Marsavina, E. Linul, T. Voiconi, D. M. Constantinescu, D. A. Apostol, On the crack path under mixed mode loading on PUR foams, Fracture and Structural Integrity, 34 (2015) 444-453.
[46] L. Marsavina, D.M. Constantinescu, E. Linul, T. Voiconi, D.A. Apostol, T. Sadowski, Evaluation of mixed mode fracture for PUR foams, Procedia Materials Science, 3 (2014) 1342-1352.
[47] E. Linul, T. Voiconi, L. Marsavina, D. Silaghi-Perju, Fracture toughness investigations of PUR foams using Asymetric Semi-Circular Bend (ASCB) specimens, Buletinul Universitatii Petrol-Gaze din Ploiesti. Seria Tehnica, LXV(4) (2014) 7-16.
[48] E. Linul, Study of the influence factors affecting the mechanical properties of rigid polyurethane foams, A PhD Thesis in Mechanical Engineering (2011).